Biochimica et Biophysica Acta 1797 (2010) 331–338

Contents lists available at ScienceDirect

Biochimica et Biophysica Acta

journal homepage: www.elsevier.com/locate/bbabio

Mechanism of strong quenching of photosystem II chlorophyll fluorescence under drought stress in a lichen, *Physciella melanchla*, studied by subpicosecond fluorescence spectroscopy

Masayuki Komura [a], Atsushi Yamagishi [a], Yutaka Shibata [a], Ikuko Iwasaki [b], Shigeru Itoh [a,*]

[a] Division of Material Science (Physics), Graduate School of Science, Nagoya University, Furocho, Chikusa, Nagoya 464-8602, Japan
[b] Faculty of Bioresource Sciences, Akita Prefectural University, Shimoshinshiro-nakano, Akita 010-0195, Japan

ARTICLE INFO

Article history:
Received 9 September 2009
Received in revised form 16 November 2009
Accepted 25 November 2009
Available online 3 December 2009

Keywords:
Chlorophyll fluorescence
Drought stress
Photosynthesis
Photosystem II
Excitation energy transfer
Lichen
Fluorescence quenching
Up-conversion spectroscopy

ABSTRACT

The mechanism of the severe quenching of chlorophyll (Chl) fluorescence under drought stress was studied in a lichen *Physciella melanchla*, which contains a photobiont green alga, *Trebouxia* sp., using a streak camera and a reflection-mode fluorescence up-conversion system. We detected a large 0.31 ps rise of fluorescence at 715 and 740 nm in the dry lichen suggesting the rapid energy influx to the 715–740 nm bands from the shorter-wavelength Chls with a small contribution from the internal conversion from Soret bands. The fluorescence, then, decayed with time constants of 23 and 112 ps, suggesting the rapid dissipation into heat through the quencher. The result confirms the accelerated 40 ps decay of fluorescence reported in another lichen (Veerman et al., 2007 [36]) and gives a direct evidence for the rapid energy transfer from bulk Chls to the longer-wavelength quencher. We simulated the entire PS II fluorescence kinetics by a global analysis and estimated the 20.2 ns^{-1} or 55.0 ns^{-1} energy transfer rate to the quencher that is connected either to the LHC II or to the PS II core antenna. The strong quenching with the 3–12 times higher rate compared to the reported NPQ rate, suggests the operation of a new type of quenching, such as the extreme case of Chl-aggregation in LHCII or a new type of quenching in PS II core antenna in dry lichens.

1. Introduction

In oxygen-evolving photosynthesis of land plants, water molecules are used as a source of electrons to fix carbon dioxide and also for transpiration [1]. Photosynthesis on land can often be risky for all terrestrial photosynthetic organisms because the excess light energy generates harmful photoproducts, such as triplet states of chlorophylls (Chls) and carotenoids, reactive oxygen species, and hydroxyl radicals, especially under drought stress. These photoproducts destroy photosystems I and II (PS I and PS II) irreversibly [2–5] and lead to cell death [6]. Some species of higher plants, algae, mosses, cyanobacteria, and lichens, however, survive even under drought environments [7–16] by relying on specific energy dissipation mechanisms. Developments of drought tolerance of photosynthetic system must have been crucial for the plants to adapt land environments.

Some lichens are highly desiccation-tolerant even under strong sunlight without a specific water-conservation mechanism [7,8]. Lichens are symbiotic organisms that contain algae and/or cyanobacteria as the photobionts inside the fungal host filaments. They grow on the ground, rocks, or trunks of trees that are often severely dehydrated at high/low temperatures. They tolerate rapid hydration/dehydration cycles as reported by Barták et al. [10] and Heber et al. [11–13], and seem to be tolerant against photoinhibition by excess light irradiation even under drought conditions [10–16]. The tolerance seems to be related to fluorescence quenching [11–16]. This resembles the nonphotochemical quenching (NPQ) mechanism of chlorophyll *a* (Chl *a*) fluorescence in the higher plants that dissipates excess solar energy into heat, although NPQ has been known to operate only under wet conditions [17–20]. The major component of NPQ is the so-called high-energy quenching, which is controlled by the xanthophyll cycle bound to LHCII antenna [17–21], and the function of PsbS subunit of PS II (20). The modulation of fluorescence yield by aggregation of LHCII is also assumed (e.g., [17–23] as detected in crystals [24] or in the LHC II aggregates [25,26]). The quenching has been proposed to occur through the energy transfer from the Chl *a* excited-singlet state to the forbidden S1 state of lutein of LHCII [26] or through the formation of a charge-transfer complex between Chl *a* and crotenoids in the antenna complexes [27–31]. It is not yet clear whether the draught-induced severe fluorescence

Abbreviations: Chl, chlorophyll; DAS, decay-associated spectrum; EET, excitation energy transfer; F_0, the fluorescence level in the dark adapted state; F_M, the fluorescence level after the saturating pulse illumination; IRF, instrument response function; LHC II, light-harvesting chlorophyll *a*/*b* binding complex II; NPQ, nonphotochemical quenching; PS, photosystem; Q_d, a quencher of excitation energy induced in the dry lichen; RC, reaction center; t_c, time constant

* Corresponding author. Tel./fax: +81 52 789 2883.
E-mail address: itoh@bio.phys.nagoya-u.ac.jp (S. Itoh).

0005-2728/$ – see front matter © 2009 Elsevier B.V. All rights reserved.
doi:10.1016/j.bbabio.2009.11.007

quenching in lichens [11–16] has a molecular mechanism common with one in the wet NPQ or not.

Chlorophyll fluorescence has been a good indicator of the activity of photosynthesis, the efficiency of light energy conversion, and the excitation energy transfer (EET). Dehydrated lichens show very low Chl *a* fluorescence with no sign of photoreaction and the addition of water rapidly recovers the Chl fluorescence and photoreactions [11–16]. The PS II fluorescence at 685 nm is known to be suppressed more severely than the 720-nm fluorescence of PS I at room temperature upon dehydration [11–16]. The fluorescence quenching mechanism in lichens functions under drought or even frozen conditions, in which xanthophyll cycle-induced NPQ mechanism does not operate well, suggesting the function of a different type of energy-dissipating mechanism.

In higher plants, the mechanism of xanthophyll cycle is known to shorten the fluorescence lifetime of PS II from 2 ns to 0.4 ns by dissipating the excess light energy into heat [32–34]. Gilmore et al. [35] reported that the lifetime of PS II fluorescence becomes shorter from 1.7 ns to 0.7 ns also in over-wintering evergreens during winter with development of a new fluorescence band centered at 715 nm (named as a cold-hard-band, CHB) at 77 K and dissipate excitation energy from PS II. Veerman et al. [36] reported that a lichen, *Parmelia sulcata*, which contains a green alga, *Trebouxia* sp., exhibited a remarkable shortening of the PS II fluorescence lifetime to 40 ps upon dehydration at room temperature. Komura et al. [37] also detected similar acceleration of decay of PS II fluorescence in dry *Physciella melanchra*. Veerman et al. proposed a chlorophyllous component that emits fluorescence at around 740 nm (Chl_{740}) as a candidate of the quencher. However, the energy influx from the bulk antenna Chls to Chl_{740} was not measured.

In the present study, we measured the fluorescence of a lichen, *Physciella melanchla*, which contains a green alga, *Trebouxia* sp., in the femtosecond to nanosecond time ranges at room temperature. We used both a streak camera and a reflection-type fluorescence up-conversion system to measure the precise kinetics and performed simulations to estimate the binding site of the quencher based on the precise rate constants of the energy transfer and energy dissipation. The drought-induced quencher(s) seems to be associated either with the peripheral LHC II or the PS II core antenna region, giving an energy dissipation rate 3–12 times higher than that estimated in the typical NPQ mechanisms in higher plants. The dehydration-induced NPQ mechanism that quenches about 90% of excitation energy in PS II seems to explain the high tolerance of lichens against severe dehydration.

2. Materials and methods

2.1. Sample preparation

Physciella melanchra (Hue.) Essl. was harvested from the trunk of a tree (*Acer buergerianum*) in the campus of Nagoya University, Nagoya, Japan. The collected thalli of the lichen were dried in the air and stored at −18 °C in a deep freezer until use. Phylogenic determination of the lichen sample was done by Dr. Y. Yamamoto (Department of Bioresource, Akita Prefectural University).

2.2. Measurements of photosynthetic activities

Changes in the flash-induced Chl *a* fluorescence yield were measured using a pulse-amplitude-modulated (PAM) fluorescence spectrometer (PAM101/102/103, Heinz Walz GmbH, Eichenring, Germany). The measuring flashlight of 10 ms at an intensity of 1 μmol photons m^{-2} s^{-1} at the sample surface was given every 1 s to monitor the fluorescence level. The F_0 and F_M levels were measured before and after additional irradiation of 3-μs red actinic light at nearly saturating intensity at 1000 mmol photons m^{-2} s^{-1} given every 30 s.

2.3. Measurements of time-resolved fluorescence

Picosecond time-resolved fluorescence spectra were measured with a streak camera spectrophotometer system as reported previously [37,38]. The excitation light was obtained from a Ti:Sapphire laser (Mai Tai; Spectra-Physics in Newport Corporation, Irvine, CA). The frequency-doubled light at 440 nm was generated by a type-I BBO crystal from an 880-nm laser pulse with a pulse duration of 150 fs and a repetition rate of 80 MHz. The laser pulse was passed through a 440-nm interference filter and focused onto the surface of the lichen thalli. The fluorescence emitted from the sample was focused by two lenses onto the entrance slit of the monochromator (50 cm Chromex 2501-S, 100 g/mm; Hamamatsu Photonics, Hamamatsu, Japan) with a slit width of 40 μm through a long-pass filter (Y-46; Toshiba, Tokyo) to eliminate the excitation laser. The spectral resolution of the system was 3.3 nm. The wavelength-dispersed fluorescence was focused onto the entrance of the streak camera (Hamamatsu 4334; Hamamatsu Photonics Inc., Hamamatsu, Japan) and then displaced as for the arriving time under a rapidly scanning electric field. The streak camera system was operated in the photon-counting mode to give 640 (wavelength) × 480 (time)-pixel 2D images. The signal was accumulated for approximately 1 h in each measurement.

Time-resolved fluorescence in the shorter time range was measured by a reflection-type fluorescence-up-conversion system [39]. Fluorescence excited by the same 440-nm laser pulse was collected in the reflective configuration from the sample surface and collimated by an off-axis paraboloidal mirror set at 90° between the excitation light and the emitted fluorescence. The collimated fluorescence beam was then passed through a long-pass filter (Y-46; Toshiba, Tokyo) and focused to a type-I BBO crystal (thickness 0.5 mm) by another paraboloidal mirror. The up-conversion light generated on the crystal was passed through a prism, focused onto the entrance slit of 10-cm monochromator (CT-10, 300 g/mm; JASCO, Tokyo) for wavelength selection, and detected by a photomultiplier (R4220; Hamamatsu Photonics, Inc., Hamamatsu). The powdered lichen thalli were fixed on a rotor of a fan that was rotated at 3000 rpm to avoid photo-damage of the sample. The excitation laser power was 18 mW (230 pJ/pulse). The spectral resolution of the up-conversion system was 10 nm. The FWHM (full width at half maximum) values of the instrument response functions (IRF) were 20 ps for the streak camera and 450 fs for the up-conversion.

2.4. Data analysis

To obtain the time-resolved fluorescence spectra at desired delay times from the streak camera image, the wavelength-time 2D fluorescence profiles obtained were divided into 96 regions of 56 ps intervals. The time courses of the fluorescence at different wavelengths were also obtained from the 2D fluorescence profiles by dividing profiles into time courses at 32 wavelength regions (20 pixels, 4.4 nm).

A global multi-exponential fitting analysis was performed on the time courses of fluorescence at all wavelength ranges. The IRF was taken into account in the convolution of the model curves to fit the fluorescence decay. The two types of time-resolved fluorescence decay curves at the same wavelength were obtained by the two different methods with different time resolutions. The decays were analyzed, respectively, to give the same number of components, time constants (t_cs), and amplitudes as done previously [38,39]. The spectral response of the up-conversion signal was calibrated in comparison with the fluorescence spectrum measured by the streak camera method at the same delay time too. The decay-associated spectrum (DAS) was calculated by plotting the amplitude of each component with the same t_c against wavelengths (for an example, see [40]).

3. Results

3.1. Effects of hydration/dehydration on the fluorescence of lichen measured by PAM

Fig. 1A shows the time course of the fluorescence yield change during the re-hydration of the desiccated *P. melanchra* thalli measured with the PAM fluorometer. Under the present experimental setup, the amplitude mainly represents the relative fluorescence yield of PS II Chls. The initial low fluorescence level (F_0) monitored by the excitation with the weak measuring flashes alone reflects the fluorescence yield when the activity of the PS II reaction center is maximal (open PS II). In the wet thallus (trace a), F_0 is high, and the actinic flash with the saturating intensity increased the fluorescence yield to the maximal level (F_M) like a spike each time. The level rapidly decreased to the F_0 level after the saturating pulse was turned off. The F_M level indicates the fluorescence yield when all the PS II reaction centers are closed. In the wet thallus, the irradiation of the continuous strong actinic light for 2 min, as shown by the up- and downward arrowheads, decreased the F_M and F_0 levels. The decrease of the level induced by the strong illumination was recovered slowly in the dark and attained the initial level again after 5 min. The responses of the wet thalli represent the typical NPQ process, as reported in algae [41,42].

Trace b in Fig. 1A shows the result in the dry thalli. The time axis represents the time after the start of re-hydration in this case. Before re-hydration, the F_0 and F_M levels were significantly low and showed almost no response to the actinic light, showing suppression of the PS II activity. Upon water addition, the F_0 level increased rapidly within a few minutes (fast rise) and then slowly to the saturated level in about 35 min (slow rise). The responses to the saturating pulses became apparent at least 1 min after the start of re-hydration, indicating the rapid recovery of PS II activity. The recovery profile upon re-hydration is similar to those reported in the wide species of drought-tolerant photosynthetic organisms, such as mosses [11], cyanobacteria [9,44] and lichens [15,16,36,37], although the times required for the recovery (1–30 min) were dependent on the species and conditions somehow.

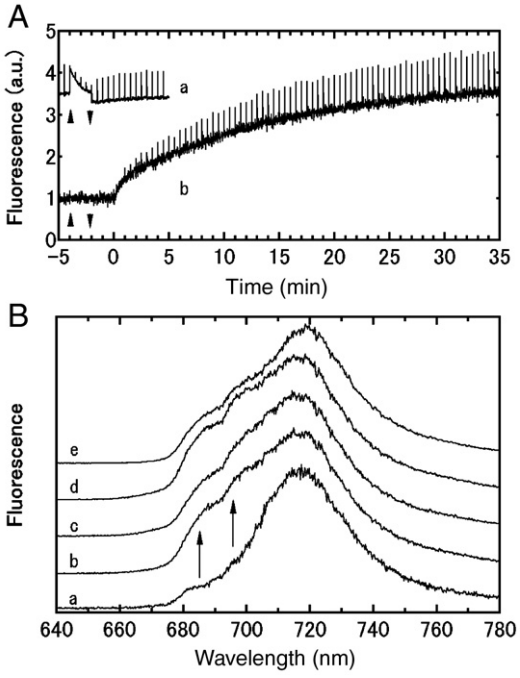

Fig. 1. A. Chlorophyll fluorescence yield measured by the PAM fluorometer of the wet (a) and dry (b) *P. melanchra* thalli. Fluorescence was measured by the repetitive monitoring flashes of low intensity as described in the text. The fluorescence yield in the dark (F_0) and just after flash pulses with saturating intensity that were provided every 30 s (F_M) was monitored. Strong continuous actinic light was provided for 2 min as indicated by down and up arrowheads. Trace a, measurement in the wet thalli. Trace b, after measuring the effects of actinic light, re-hydration was started by adding water at 0 min. B. Steady-state fluorescence spectra at 77 K of the dry thalli (trace a) and thalli frozen at 30 s (trace b), 1 min (trace c), 10 min (trace d), and 30 min (trace e) after the start of re-hydration. The excitation wavelength was 440 nm. Spectra were normalized at their respective highest peaks. The arrows represent the positions of PS II fluorescence bands at 685 and 695 nm.

3.2. Effects of re-hydration on the 77K steady-state fluorescence spectra

Dry *P. melanchra* thalli with water added were rapidly frozen in liquid nitrogen, and their fluorescence spectra were measured at 77 K with 440-nm excitation light (Fig. 1B). At 30 min after the start of the re-hydration the lichen (trace e in Fig. 1B) gave a fluorescence peak at 720 nm, which is assigned to be emitted from the red Chls in PS I, at 685 and 695 nm from the PS II Chls. Hereafter, we designate the fluorescence band at 720 nm that belongs to PS I as F720 and those at 685 and 695 nm as F685 and F695, respectively. Trace a in the dry lichen showed a large PS I fluorescence band at 718 nm (slightly blue-shifted from 720 nm) and almost negligible PS II bands at 680–700 nm. The re-hydration enhanced all the PS II bands gradually and shifted the PS I band to 720 nm with a slight increase of intensity as seen in b–d traces. The results are in agreements with those reported in the re-hydration process of drought-tolerant cyanobacteria at 77 K [43,44], mosses, and lichens at room temperature [11,12,15]. After hydration for 30 s, the F685 and F695 bands increased, as indicated by arrows. No peak shifts were detected in these PS II bands. The results indicate that the desiccation/re-hydration process more significantly affected the PS II fluorescence bands. This observation is in agreement with the fast increase in F_0 and F_m levels observed by the PAM measurement. PS II that has been inactive with a very low fluorescence yield in the dry lichen, thus, seems to regain the electron transfer activity rapidly after the re-hydration.

3.3. Picosecond fluorescence kinetics at room temperature

We measured the picosecond time-wavelength-2D image of the fluorescence kinetics using the streak camera system at room temperature as described in Materials and methods. Fig. 2A and B represents the images obtained in the wet and dry lichen thalli, respectively, after excitation by a 150-fs laser pulse at 440 nm. The spectral widths of the images along the horizontal axes are not very much different from each other; the decays of fluorescence that are judged from the tails along the vertical axes were very different. In the wet thalli, we see the long decay over 3 ns of 680–90 nm band, while only a short decay within a few tenths of nanosecond in the dry thalli. The images clearly indicate that the fluorescence decay in this time range is significantly shortened in the dry lichen as reported previously [36,37].

Fig. 2C and D shows the normalized time-resolved spectra measured at 2–776 ps in wet and dry thalli. They gave a fluorescence peak at 685 nm with a broad shoulder at around 740 nm. In the wet thalli (A and C), the 710 nm PS I shoulder peak decayed faster than the 685 nm peak of PS II fluorescence that remained even at 776 ps. In the dry thalli, the spectrum at 2 ps was similar. However, the whole decay is accelerated due to the faster 685-nm decay.

Fig. 3 shows the fluorescence decay kinetics at selected wavelengths in the wet and dry thalli for 800 ps. In the wet thalli (Fig. 2A), the fluorescence at 710 nm decayed faster than that at 680 and 740 nm. The rapid decay at 710 nm can be estimated to represent the fast decay of the PS I fluorescence. The PS II fluorescence at 680 nm decayed more slowly. On the other hand, in the dry thalli, the Chl fluorescence lost slow components and decayed much faster especially at the shorter wavelength region as shown in Fig. 3B. The results suggest the fluorescence quenching in PS II of the dry lichen as proposed previously [36,37].

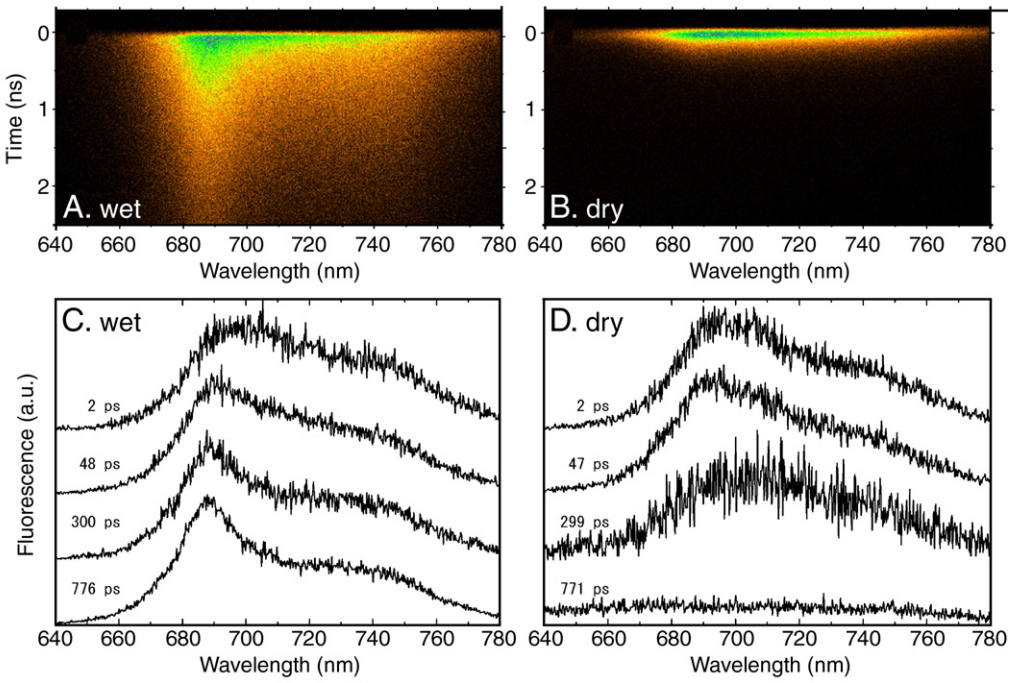

Fig. 2. Time-wavelength 2D images and time-resolved spectra of fluorescence measured by the streak camera system in dry and wet thalli of *P. melanchra* at room temperature. A, image of wet thalli. B, image of dry thalli. C and D, time-resolved fluorescence emission spectra in the wet and dry thalli, respectively. Each spectrum was normalized at its maximum peak. See Materials and methods for the details of the measuring conditions. Fluorescence was excited by a 440 nm laser pulse of 150 fs.

3.4. Effects of hydration/dehydration on the fluorescence kinetics in subpicosecond time domain

We applied the fluorescence up-conversion technique to investigate the fluorescence kinetics in the shorter subpicosecond time domain. Fig. 4A and B shows the fluorescence time courses in the wet and dry thalli, respectively, at various wavelengths within 25 ps. The kinetics within 5 ps was measured with short time intervals of 0.027 ps and that after 5 ps was with longer 0.27 ps intervals to measure the rise and decay precisely. In the wet thalli, the fluorescence at 684 nm showed a decay slower than that at 713 nm. The fluorescence at 728 and 743 nm showed a small rise. The rising phases detected above 713 nm are likely to reflect the EET from bulk Chls to the red Chl species in PS I.

In the dry thalli, fluorescence decays were faster even in this short time range than those in the wet ones, especially at 684 nm. The kinetics at 713, 728 and 743 nm showed clear fast rising phases, whereas the kinetics at 684 nm gave no rising phase (Fig. 4B). This implies the fast EET from the 684-nm Chls to the longer-wavelength ones also in the dry thalli. The kinetics up to 60 ps at 713–743 nm are a little faster but not significantly different from those in the wet thalli, suggesting that EET from the bulk to the red Chls in PS I was not significantly affected.

3.5. Global multi-exponential analysis of fluorescence kinetics in subpicosecond to nanosecond timescale

Fluorescence time courses at the same range of wavelength were measured both by the streak camera method and the fluorescence up-conversion method in the long and short time ranges. The dataset at each wavelength range obtained by the two methods was analyzed globally to fit the multi-exponential model function, as described in Materials and methods. We assumed a set of four kinetic components to fit all the fluorescence kinetics measured under the wet condition. Another set was assumed for kinetics under the dry condition. The decay-associated spectrum (DAS) was calculated from the amplitudes

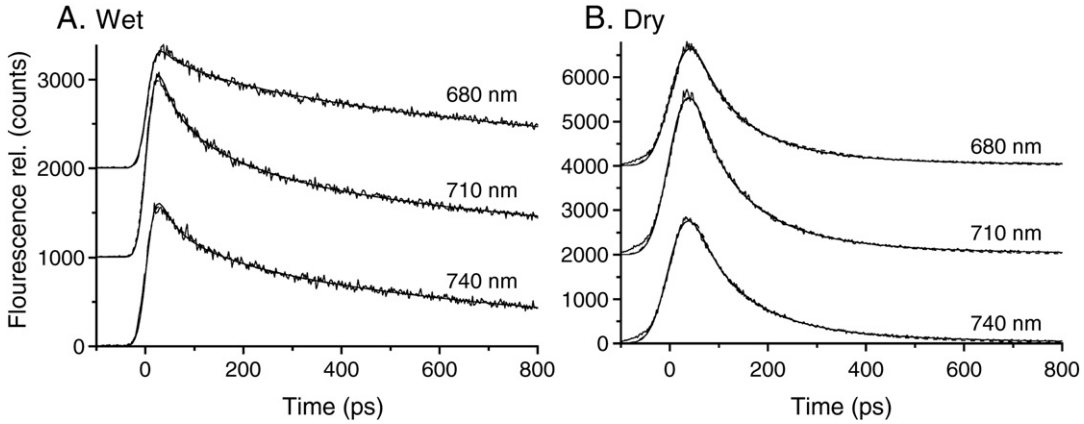

Fig. 3. Fluorescence decay curves of the wet (A) and dry (B) *P. melanchra* thalli at room temperature obtained from images measured by the streak camera system. The detection wavelengths were 680, 710, and 740 nm, as indicated. Smooth solid lines represent the fitting curves calculated by the global multi-exponential decay analysis, and the dashed lines, the fitting curves by the target analysis, based on the compartment model described in Fig. 5. See text for details of the analysis. The data were obtained from a data set in Fig. 3.

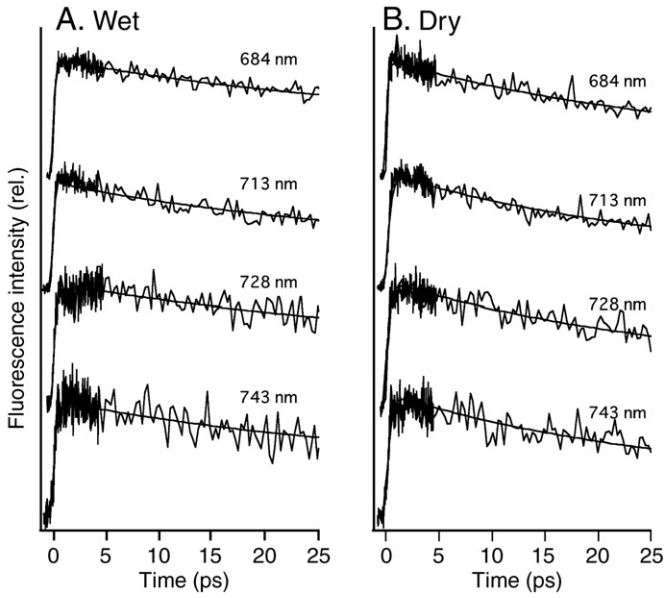

Fig. 4. Fluorescence decay curves of the wet (A) and dry (B) *P. melanchra* thalli at room temperature measured by the fluorescence up-conversion method excited by a 440 nm laser pulse of 150 fs. The detection wavelengths were 684, 713, 728, and 743 nm, as indicated. Smooth lines represent the fitting curves calculated by the global multi-exponential analysis. The time intervals between the measuring points were 0.027 ps and 0.27 ps before and after 5 ps, respectively. See text for details.

at different wavelengths of the kinetic phase with the same t_c, as shown in Fig. 5.

In the wet thalli, the fastest DAS component showed a t_c of 0.72 ps. This component had negative amplitudes at 700 and 730 nm. The spectral shape suggests the EET from the bulk Chls to the red Chl bands at 700 and 730–740 nm in PS I, although the t_c is somewhat shorter than those reported in cyanobacterial and plant PS I [45–48]). The relatively small contributions of the fastest component to the overall decay kinetics seem to be partially due to the overlap of PS II fluorescence. The fast internal conversion from the Soret band to the Q_y band of the bulk Chls with estimated t_cs of around 0.1 ps may also contribute to this phase. The second component with a 32 ps t_c showed a broad positive band above 683 nm, indicating the fast decay of fluorescence. This t_c value is very close to the major decay time constant of fluorescence reported in the isolated PS I–LHC I super complex of several organisms [45–52]. The third component with a t_c of 144 ps is small and also seems to represent a contribution from PS I, judging from its peak wavelength and short t_c value. The slowest component with a t_c of 934 ps had a broad positive band at 683–740 nm and seems to represent EET in PS II. The t_c value is longer than that expected for the fully open PS II RC traps [53–57], and the spectral shape is somewhat more extended to the wavelength range of PS I that is longer than the range of PS II Chls. This implies that a significant portion of PS II RC that was in the closed state contributed to the slow decay kinetics [34,35,53–57] and that this phase is overlapped by the slow decay components of PS I Chls above 700 nm as well.

The dry thalli showed a very large negative DAS component with a very short t_c of 0.31 ps that is two times faster than that of the fastest one detected in the wet thalli. Its spectrum had negative peaks at 713 and above 743 nm, and the amplitudes were significantly larger than that of negative 0.72-ps component detected in the wet thalli. The negative 0.31-ps DAS suggests the rapid influx of excitation energy to the longer-wavelength Chls. The second and third components gave t_c values of 23 ps and 112 ps, respectively, giving broad featureless positive spectra with an apparent peak at around 700 nm, indicating the rapid dissipation of the excitation energy. The spectra are similar to those in the 32 and 943 ps DAS components in the wet thalli in Fig. 4A. It is likely that PS I gives almost the same DAS spectra at room temperature in both the wet and dry thalli because we observed only a 2-nm blue-shift of the PS I red Chl peak in the dry thalli at 77 K in Fig. 1B. The DAS spectra in Fig. 5B in the dry thalli, however, are somewhat different from the pure PS I or PS II spectrum, and, thus, seem to represent a mixture of PS I and PS II DASs that may give t_c values at around 23 and 112 ps. It is clear that the PS II fluorescence decay time that was mainly 934 ps in the wet condition is drastically shortened due to some quenching process triggered by drying.

A small positive component with the slowest 362-ps t_c in the dry thalli gave a broad positive spectrum with an apparent peak at 730 nm. The contribution of the component to the whole decay is almost negligible, and this component does not seem to have its counterpart in the fluorescence kinetics of the wet thalli. No slower component was detected in the dry thalli, indicating that most of the excitation energy in PS II is dissipated with 23-ps and 112-ps t_c phases. The loss of longer component interprets the drought-induced decrease in the steady-state fluorescence as seen in Fig. 1.

The results obtained in this study directly indicate the fast 0.31 ps EET from the bulk PS II Chls to the longer-wavelength bands. The feature of kinetics in the longer time scale is almost similar to those reported previously [37] or by Veerman et al. [36] who observed the shortening of the decay t_c of PS II fluorescence in *P. sulcata* to 40 ps upon dehydration, though the 0.72- and 0.31-ps DAS components could not be resolved in the previous studies.

4. Discussion

4.1. Function of a quencher

Lichens have been known to stop photoreactions and to show suppressed Chl *a* fluorescence under drought conditions [11–16], in which xanthophyll cycle-induced fluorescence quenching does not

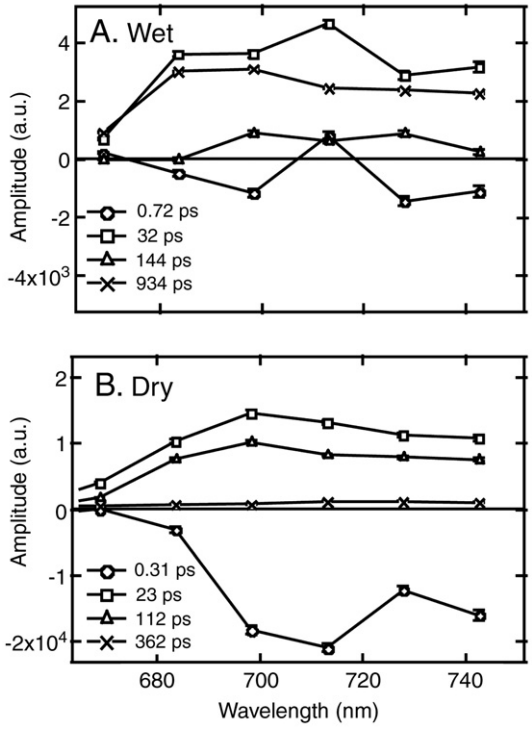

Fig. 5. Decay-associated spectra (DAS) calculated by the global multi-exponential analysis of the fluorescence decay curves measured by the streak camera and the fluorescence up-conversion methods in the wet (A) and dry (B) thalli of *P. melanchra.* The time constant for each DAS is shown in the figure. See text for details.

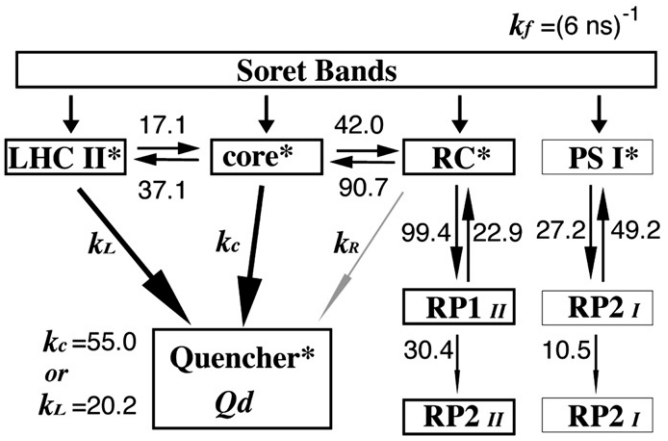

Fig. 6. Compartment model and estimated quenching rate of the excitation energy in PS II in the dry thalli of *P. melanchra*. Rate constants are shown in the unit of ns^{-1}. See text for details.

operate as reported by Kopecky et al. [30]. The drought-induced fluorescence quenching suggests the operation of an energy dissipation mechanism that is different from ordinary NPQ that occurs only under wet conditions. Veerman et al. [36] reported the fast decay of fluorescence at 740 nm with a t_c of 40 ps in the picosecond fluorescence measurement of a dry lichen, *P. sulcata*, and designated the quencher as Chl_{740}. In the present study, we measured the femtosecond fluorescence kinetics using the reflection-mode fluorescence up-conversion and streak camera systems. The results give a direct evidence for the accumulation of excitation energy with a short 0.31-ps t_c and its rapid dissipation with t_c values of 23 and 112 ps accompanied with weak fluorescence above 700 nm from a green algal photobiont, *Trebouxia* sp., inside a dry lichen *P. melanchla*. We designated the quencher molecule to be "Q_d" in this paper, rather than Chl_{740}, because the fast 0.31-ps DAS gave a rather broad spectrum peaking at 715 and above 740 nm, and its molecular identity is not clear yet. The peak around 715 nm in DAS also resembles the CHB (cold-hard-band) fluorescence at 715 nm detected in the overwintering evergreens reported by Gilmore et al. [35] or the far-red fluorescence bands indicated in the NPQ studies [17,25] too. Subpicosecond measurements at cryogenic temperatures with a carefully selected sample might give the better spectral and kinetic features of Q_d.

We obtained DAS with a t_c of 0.31 ps with large negative peaks at 713 and above 740 nm and DAS with t_c values of 23 and 112 ps with positive amplitudes above 700 nm in the dry lichen. The results suggest the 0.31-ps energy accumulation to Q_d from the bulk PS II Chls and the dissipation of excitation energy with a time constant at around 23–112 ps with weak fluorescence emission above 700 nm. The emission was almost negligible in the steady-state fluorescence spectra at 77 K both under wet and dry conditions (Fig. 1B). This suggests the fast non-radiative transition to the ground state from Q_d, which has the lowest energy level, compared to all the Chl levels in PS II. The red Chls in LHC I cannot be Q_d because the far-red fluorescence from LHC I was not significantly affected by the hydration/dehydration of lichen. The location of Q_d that is active only under a drought condition was assumed to be either on LHCII or on the PS II core based on a global multi-exponential decay analysis, as shown below in the present study.

In PS I the increased charge recombination between A_1^- and $P700^+$ under drought stress was suggested to prevent the photo-damage of lichens by Bukhov et al. [31]. The loss of water molecules in PS I induced the 2–3 nm blue-shift of the PS I fluorescence peak of red Chls at 77 K as seen in Fig. 1B and made the fluorescence decay of PS I at room temperature a little faster by depleting the slow phase. These effects might protect PS I from photo-damage too.

4.2. Kinetic modeling and simulation of fluorescence kinetics in dry lichen

We formulated a model to describe the fluorescence kinetics (Fig. 6) in order to evaluate the experimental results. We assumed a simple model consisting of three compartments in PS II. The three compartments LHC II*, core*, and RC* represent the peripheral antenna complex, the unified compartment of CP43 and 47, and the active reaction center of PS II, respectively, with the excitation energy on their Chls. The three compartments exchange the excitation energy to each other with intrinsic EET rates. RC* is further connected to the two radical-pair states ($RP1_{II}$ and $RP2_{II}$) with three intrinsic electron transfer (ET) rates, as shown in Fig. 6. This model is based on the one used by Miloslavina et al. [54], Broess et al. [55] and Raszewski and Renger [57], and is the simplest among the several models previously proposed for the ET process in PS II. We added another compartment for the quencher "Q_d," in PS II to interpret the observed rapid fluorescence decay in the dry lichen. We examined three models in which Q_d is connected to the LHC II*, core*, and RC* compartment, respectively. We also added PS I together with three compartments, namely, PS I*, $RP1_I$, and $RP2_I$. Inside PS I, we did not consider the EET to simplify the model, and we used the reversible radical-pair model used by Holzwarth et al. [46].

We made basic five assumptions as below to simplify the analysis. (1) All the intrinsic EET rates for the three compartments, LHC II*, core*, and RC*, are almost equal to their counterparts in the plant PS II with almost the same fluorescence spectra at room temperature. (2) A PS I to PS II ratio is 1.0. (3) The ET rates in PS I and II are unaffected by dehydration. (4) The fluorescence spectrum of PS I is unaffected by dehydration. (5) The excitation energy is equilibrated among Q_d and the Chls in three compartments and Q_d converts the excitation energy to heat rapidly with almost no emission of fluorescence. We added the term k_f of (6 ns)$^{-1}$ to represent the rate constant for the radiative relaxation to the ground state of Chls.

By fitting the fluorescence decay data obtained in the isolated BBY-type PS II membranes at room temperature according to Broess et al. [55] we first determined the EET rates among LHC II*, core*, and RC* together with all the ET rates in spinach PS II (Fig. S1). The amounts of Chls bound to LHC II*, core*, and RC* were estimated as 111, 29, and 8 (148 in total), respectively, according to Broess et al. [55] and references therein. The model, therefore, simulated the PS II fluorescence decay curve successfully (Fig. S1B, and also summarized in Fig. S2). The estimated EET rates among three compartments were essentially similar to those reported [54,55,57], indicating the validity of the present model.

We secondly estimated the ET rates in PS I and PS II in the wet lichen thalli. As shown by dashed lines in Fig. 3A, the model successfully reproduced the whole fluorescence kinetics with ET and

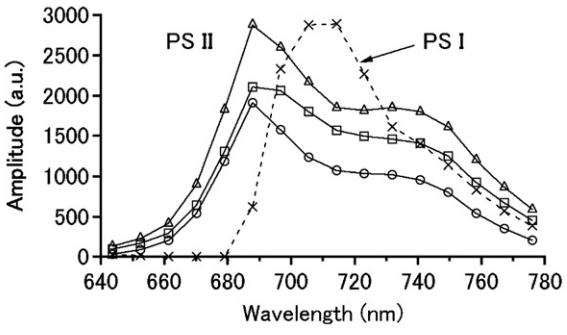

Fig. 7. Species-associated spectra (SAS) of PS I and II calculated by the target analysis. SAS of PS II in the wet condition (circle), of PS I in the wet condition (cross), of PS II in the dry condition when the excitation energy is assumed to be quenched in the core part (square) or in the LHC II part (triangle). See text for details.

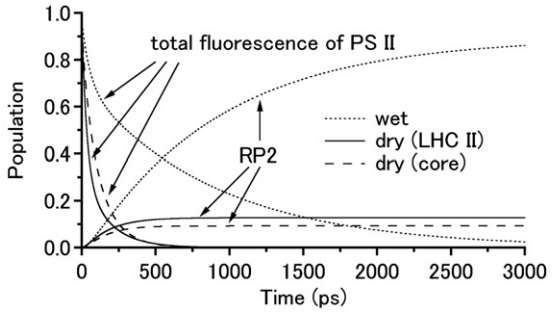

Fig. 8. Time evolution of the population of the excitation energy in PS II or in the RP2 state in the wet and dry lichens.

EET rates as summarized in Fig. 6. The effective rate estimated for the primary charge separation in PS I was almost comparable to that reported for plant PS I by Holzwarth et al. [46] and Slavov et al. [48]. The estimated forward ET rates in PS II, were slower, whereas the backward ones were a little faster than those estimated for spinach PS II (Fig. 2 in SI). The difference seems to be explained by assuming the PS II trap in the wet thalli to be partially closed under the high excitation energy of laser used for the up-conversion measurement. Fig. 7 shows the calculated species-associated fluorescence spectra (SAS) of PS I and II. The PS II fluorescence spectrum (a line with circles) had a peak at around 690 nm and a large shoulder at around 740 nm. The PS I fluorescence spectrum had a peak at around 710 nm with a broad bandwidth (a dashed line with crosses). The spectrum roughly corresponds to the 32- and 144-ps DASs in the wet lichen (Fig. 5A) and seems to mainly represent the fluorescence decay of PS I.

We attempted to reproduce the measured fluorescence kinetics of the dry lichen by three different models that assumed the energy dissipation by Q_d to take place in one of the three compartments in PS II based on the parameters obtained from the simulations in the isolated PS II and the wet lichen above. All three of the models reproduced the actual fluorescence decay curves well. The dashed lines in Fig. 3B represent the model curves based on the LHC II-dissipation model as an example. However, the RC-dissipation model gave an extremely high quenching rate (k_R) of over 10,000 ns^{-1}. The k_L value estimated in the LHC II-dissipation model and the k_C value in the core-dissipation model are 20.2 and 55.0 ns^{-1}, respectively. The different quenching rates are explained by a shift of equilibration of the excitation energy between the compartments, as shown in Fig. 6.

4.3. Location of the quencher Q_d and its function mechanism

Although all three models reproduced the observed fluorescence kinetics well, the RC-dissipation model can be excluded because of the unrealistic quenching rate constant (k_R) of over 10,000 ns^{-1}. The rate constants estimated for the LHC II-dissipation and core-dissipation models (20 and 55 ns^{-1}, respectively) seem possible under some situations because they are from three to a maximum of 12 times higher than the NPQ-type quenching rate reported in higher plants (e.g., 4.6 ns^{-1} assumed by Holt et al. [29]; 6.7 ns^{-1} by Ruban et al. [27]; and 4.8 ns^{-1} by Miloslavina et al. [25]). Thus, Q_d seems to be very strongly coupled either to the core or to LHC II Chls and to realize a very efficient quenching that can decrease even the F_0 level significantly. The high shoulders at 720–740 nm in the calculated SAS of PS II of lichen in Fig. 7 seem to include the weak fluorescence emission from Q_d.

Some NPQ mechanisms predicted modification of LHCII state [18,19,24–29]. Models assume the energy transfer to a carotenoid from LHC [26,27], to the oligomers of LHC II [24,26–28] or to the broad charge-transfer (CT) band between Chl and carotenoid above 700 nm [28–30]. The CHB band detected in the winter plants [35] might also be produced by similar mechanism. The reported quenching rate constant induced by the LHC II oligomerization or CHB-quenching was 5–7 ns^{-1} [19,21,35] and is significantly lower than the high rate constant of 20 ns^{-1} estimated in the LHCII-dissipation model in dry lichen in this study. The core-dissipation model, on the other hand, predicts the higher 55 ns^{-1} rate for k_C and estimates 90% dissipation of the excitation energy (Fig. 8). The model can interpret the observed quenching of F684/F695 detected at 77 K well (Fig. 1B).

Although we cannot determine the precise location of the quencher at present, its quenching efficiency is higher than that reported for the known NPQ mechanisms. We, therefore, assume it to occur by a new mechanism, such as the extreme case of Chl-aggregation-induced quenching in the dried Chl-proteins under special environments. The quencher in lichen that has absorption/emission above 715 nm might be either an exciton band of aggregated Chls or CT band between Chl *a* and carotenoid produced by the modification of the structure of LHC II or CP43/CP47 proteins. If LHC II is responsible for the draught-induced nonphotochemical quenching (d-NPQ) in lichen, it might come from the extremely strong interaction between the pigments in the dried LHC II. The quenching, then, might occur through a molecular mechanism that is essentially similar to the one in wet NPQ. If d-NPQ occurs in CP43/CP47 proteins, we should think of a new model, which assumes the draught-induced modification of pigment interaction in the CP43/CP47 proteins. This might interpret the quenching in cyanobacteria [9] too. The contribution from the fungal side seems to be also important because the isolated photobiont green alga is reported to partially lose their drought tolerance [12] and because the dried spinach PS II particles did not show d-NPQ (Komura et al., unpublished results).

Elucidation of the mechanism of the d-NPQ will yield new perspectives for the regulation of photosynthetic energy conversion. The d-NPQ mechanism that is distributed among a wide variety of lichens, algae and cyanobacteria might have been important also for the land-invasion process of photosynthesis.

Acknowledgments

This work was supported by a Grant-in-Aid (No. 19370064) from the Japanese Ministry of Education, Science, Sports, and Culture to S.I. We are grateful to Dr. Y. Yamamoto (Department of Bio-Resource, Akita Prefectural University) for the taxonomic determination of the lichen species and valuable discussions during the work.

Appendix A. Supplementary data

Supplementary data associated with this article can be found, in the online version, at doi:10.1016/j.bbabio.2009.11.007.

References

[1] N. Nelson, C.F. Yocum, Structure and function of photosystems I and II, Ann. Rev. Plant Biol. 57 (2006) 521–565.
[2] K. Satoh, D.C. Fork, Photoinhibition of reaction centers of photosystems I and II in intact *Bryopsis* chloroplasts under anaerobic conditions, Plant Physiol. 70 (1982) 1004–1008.
[3] J. Barber, B. Andersson, Too much of a good thing, light, can be bad for photosynthesis, Trends Biochem. Sci. 17 (1992) 61–66.
[4] N. Smirnoff, The role of active oxygen in the response of plants to water deficit and desiccation, New Phytol. 125 (1993) 27–58.
[5] K. Sonoike, Photoinhibition of photosystem I: its physiological significance in the chilling sensitivity of plants, Plant. Cell. Physiol. 37 (1996) 239–247.
[6] V. Shuvalov, U. Heber, Photochemical reactions in dehydrated photosynthetic organisms, leaves, chloroplasts and photosystem II particles: reversible reduction of pheophytin and chlorophyll and oxidation of β-carotene, Chem. Phys. 294 (2003) 227–237.
[7] K. Palmqvist, Carbon economy in lichens, New Phytol 148 (2000) 11–36.
[8] F.A. Hoekstra, E.A. Golovina, J. Buitink, Mechanisms of plant desiccation tolerance, Trends Plant Sci. 9 (2001) 431–438.
[9] K. Satoh, M. Hirai, J. Nishio, T. Yamaji, Y. Kashino, H. Koike, Recovery of photosynthetic systems during rewetting is quite rapid in a terrestrial cyanobacterium, *Nostoc commune*, Plant Cell. Physiol. 43 (2002) 170–176.

[10] M. Barták, J. Gloser, J. Hájek, Visualized photosynthetic characteristics of the lichen *Xanthoria elegans* related to daily courses of light, temperature and hydration: a field study from Galindez Island, maritime Antarctica, The Lichenologist 37 (2005) 433–443.
[11] U. Heber, W. Bilger, V.A. Shuvalov, Thermal energy dissipation in reaction centers and in the antenna of photosystem II protects desiccated poikilohydric mosses against photo-oxidation, J. Exp. Bot. 57 (2006) 2993–3006.
[12] U. Heber, V.A. Shuvalov, Photochemical reactions of chlorophyll in dehydrated photosystem II: two chlorophyll forms (680 and 700 nm), Photosyn. Res. 84 (2005) 85–91.
[13] U. Heber, O.L. Lange, V.A. Shuvalov, Conservation and dissipation of light energy as complementary processes: homoiohydric and poikilohydric autotrophs, J. Exp. Bot. 57 (2006) 1211–1223.
[14] I. Kranner, W.J. Cram, M. Zorn, S. Wornik, I. Yoshimura, E. Stabentheiner, H. Pfeifhofer, Antioxidants and photoprotection in a lichen as compared with its isolated symbiotic partners, Proc. Natl. Acad. Sci. U. S. A. 102 (2005) 3141–3146.
[15] J. Kopecky, M. Azarkovich, E.E. Pfündel, V.A. Shuvalov, U. Heber, Thermal dissipation of light energy is regulated differently and by different mechanisms in lichens and higher plants, Plant Biol. 7 (2005) 156–167.
[16] N.G. Bukhov, S. Govindachary, E.A. Egorova, R. Carpentier, Recovery of photosystem I and II activities during re-hydration of lichen *Hypogymnia physodes* thalli, Planta 219 (2004) 110–120.
[17] P. Horton, A.V. Ruban, R.G. Walters, Regulation of light harvesting in green plants, Annu. Rev. Plant Mol. Biol. 47 (1996) 655–684.
[18] B. Demmig-Adams, Carotenoids and photoprotection in plants: a role for the xanthophyll zeaxanthin, Biochim. Biophys. Acta 1020 (1990) 1–24.
[19] A.V. Ruban, A.J. Young, P. Horton, Modulation of chlorophyll fluorescence quenching in isolated light harvesting complex of photosystem II, Biochim. Biophys. Acta 1186 (1994) 123–127.
[20] K.K. Niyogi, Photoprotection revisited: genetic and molecular approaches, Annu. Rev. Plant Physiol. Plant Mol. Biol. 50 (1999) 333–359.
[21] A.V. Ruban, P. Horton, The xanthophyll cycle modulates the kinetics of nonphotochemical energy dissipation in isolated light-harvesting complexes, intact chloroplasts, and leaves of spinach, Plant Physiol. 119 (1999) 531–542.
[22] R.C. Jennings, F.M. Garlaschi, G. Zucchelli, Light-induced fluorescence quenching in the light-harvesting chlorophyll a/b protein complex, Photosynth. Res. 27 (1991) 57–64.
[23] V. Barzda, R.C. Jennings, G. Zucchelli, G. Garab, Kinetic analysis of the light-induced fluorescence quenching in light-harvesting chlorophyll *a*/*b* pigment–protein complex of Photosystem II, Photochem. Photobiol. 70 (1999) 751–759.
[24] Z.F. Liu, H.C. Yan, K.B. Wang, T.Y. Kuang, J.P. Zhang, J. Wang, Crystal structure of spinach major-light harvesting complex at 2.72Å resolution, Nature 428 (2004) 287–292.
[25] Y. Miloslavina, A. Wehner, P.H. Lambrev, E. Wientjes, M. Reus, G. Garab, R. Croce, A.R. Holzwarth, Far-red fluorescence: a direct spectroscopic marker for LHC II oligomer formation in non-photochemical quenching, FEBS Lett. 582 (2008) 3625–3631.
[26] A.A. Pascal, Z. Liu, K. Broess, B. van Oort, H. van Amerongen, C. Wang, P. Horton, P. B. Robert, W. Chang, A. Ruban, Molecular basis of photoprotection and control of photosynthetic light-harvesting, Nature 436 (2005) 134–137.
[27] A.V. Ruban, R. Berera, C. Illioaia, I.H.M. van Stokkum, T.M. Kennis, A.A. Pascal, H. van Amerongen, B. Robert, P. Horton, R. van Grondelle, A mechanism of photoprotective energy dissipation in higher plants, Nature 450 (2007) 575–578.
[28] T.K. Ahn, T. Avenson, M. Ballottari, Y.C. Cheng, K.K. Niyogi, R. Bassi, G.R. Fleming, Architecture of a charge-transfer state regulating light harvesting in a plant antenna protein, Science 320 (2008) 794–797.
[29] N.E. Holt, G.R. Fleming, K.K. Niyogi, Toward an understanding of the mechanism of non-photochemical quenching in green plants, Biochem. 43 (2004) 8281–8289.
[30] N.E. Holt, D. Zigmantas, L. Valkunas, X. Li, K.K. Niyogi, G.R. Fleming, Carotenoid cation formation and the regulation of photosynthetic light harvesting, Science 307 (2005) 433–436.
[31] R. van Grondelle, J.P. Dekker, T. Gillbro, V. Sundstrom, Energy trapping and transfer in photosynthesis, Biochim. Biophys. Acta 1187 (1994) 1–65.
[32] A.M. Gilmore, T.L. Hazlett, Govindjee, Xanthophyll cycle-dependent quenching of photosystem II chlorophyll *a* fluorescence: formation of a quenching complex with a short fluorescence lifetime, Plant Biol. 92 (1995) 2273–2277.
[33] A.M. Gilmore, V.P. Shinkarev, T.L. Hazlett, Govindjee, Qualitative analysis of the effects of intrathylakoid pH and xanthophyll cycle pigments on chlorophyll *a* fluorescence lifetime distributions and intensity in thylakoids, Biochem. 37 (1998) 13582–13593.
[34] M. Richter, R. Goss, B. Wagner, A.R. Holzwarth, Characterization of the fast and slow reversible components of non-photochemical quenching in isolated pea thylakoids by picosecond time-resolved chlorophyll fluorescence analysis, Biochem. 38 (1999) 12718–12726.
[35] A.M. Gilmore, S. Matsubara, M.C. Ball, D.H. Barker, S. Itoh, Excitation energy flow at 77 K in the photosynthetic apparatus of overwintering evergreens, Plant Cell Environ. 26 (2003) 1021–1034.
[36] J. Veerman, S. Vasil'ev, G.D. Paton, J. Ramanauskas, D. Bruce, Photoprotection in the lichen *Parmelia salcata*: the origins of desiccation-induced fluorescence quenching, Plant Physiol. 145 (2007) 997–1005.
[37] M. Komura, M. Iwasaki, S. Itoh, Drought-induced ultra-fast fluorescence quenching in photosystem II in lichens revealed by picosecond time-resolved fluorescence spectrophotometry, in: J.F. Allen, E. Gantt, J.H. Golbeck, B. Osmond (Eds.), Photosynthesis, Energy From the Sun: 14th International Congress on Photosynthesis, Springer, 2008, pp. 1023–1026.
[38] M. Komura, Y. Shibata, S. Itoh, A new fluorescence band F689 in photosystem II revealed by picosecond analysis at 4-77 K: function of two terminal energy sinks F689 and F695 in PS II, Biochim. Biophys. Acta 1757 (2006) 1657–1668.
[39] Y. Shibata, Y. Murai, Y. Satoh, Y. Fukushima, K. Okajima, M. Ikeuchi, S. Itoh, Acceleration of electron-transfer-induced fluorescence quenching upon conversion to the signaling state in the blue-light receptor, TePixD, from *Thermosynechococcus elongatus*, J. Phys. Chem. B 113 (2009) 8192–8198.
[40] I.H.M. van Stokkum, B. van Oort, F. van Mourik, B. Gobets, H. van Amerongen, (Sub)-picosecond spectral evolution of fluorescence studied with a synchroscan streak-camera system and target analysis, in: T.J. Aartsma, J. Matysik (Eds.), Biophysical Techniques in Photosynthesis (Advances in Photosynthesis and Respiration, Vol 26), Springer, Dordrecht, 2008, pp. 223–240.
[41] U. Schreiber, C. Neubauer, U. Schliwa, PAM fluorometer based on medium-frequency pulsed Xe-flash measuring light: a highly sensitive new tool in basic and applied photosynthesis research, Photosyn. Res. 36 (1993) 65–72.
[42] C. Casper-Lindley, O. Björkman, Fluorescence quenching in four unicellular algae with different light-harvesting and xanthophyll-cycle pigments, Photosyn. Res. 56 (1998) 277–289.
[43] Y. Harel, I. Ohad, A. Kaplan, Activation of photosynthesis and resistance to photoinhibition in cyanobacteria within biological desert crust, Plant Physiol. 143 (2004) 3070–3079.
[44] I. Ohad, R. Nevo, V. Brumfeld, Z. Reich, T. Tsur, M. Yair, A. Kaplan, Inactivation of photosynthetic electron flow during desiccation of desert biological sand crusts and *Microcoleus* sp.-enriched isolates, Photochem. Photobiol. Sci. 4 (2005) 977–982.
[45] B. Gobets, I.H.M. van Stokkum, M. Rögner, J. Kruip, E. Schlodder, N.V. Karapetyan, J.P. Dekker, R. van Grondelle, Time-resolved fluorescence emission measurements of photosystem I particles of various cyanobacteria: a unified compartment model, Biophys. J. 81 (2001) 407–424.
[46] A.R. Holzwarth, M.G. Muller, J. Niklas, W. Lubitz, Charge recombination fluorescence in photosystem I reaction centers from *Chlamydomonas reinhardtii*, J. Phys. Chem. B 109 (2005) 5903–5911.
[47] J.A. Ihalainen, I.H.M. van Stokkum, K. Gibasiewicz, M. Germano, R. van Grondelle, J.P. Dekker, Kinetics of excitation trapping in intact photosystem I of *Chlamydomonas reinhardtii* and *Arabidopsis thaliana*, Biochim. Biophys. Acta 1706 (2005) 267–275.
[48] C. Slavov, M. Ballottari, T. Morosinotto, R. Bassi, A.R. Holzwarth, Trap-limited charge separation kinetics in higher plant photosystem I complexes, Biophys. J. 94 (2008) 3601–3612.
[49] R. Croce, D. Dorra, A.R. Holzwarth, R.C. Jennings, Fluorescence decay and spectral evolution in intact photosystem I of higher plants, Biochem. 39 (2000) 6341–6348.
[50] A.N. Melkozernov, J. Kargul, S. Lin, J. Barber, R.E. Blankenship, Energy coupling in the PS I-LHCI supercomplex from the green alga *Chlamydomonas reinhardti*, J. Phys. Chem. B 108 (2004) 10547–10555.
[51] E. Engelmann, G. Zucchelli, A.P. Casazza, D. Brogioli, F.M. Garlaschi, R.C. Jennings, Influence of the photosystem I-light harvesting complex I antenna domains on fluorescence decay, Biochem. 45 (2006) 6947–6955.
[52] Y. Ikeda, M. Komura, M. Watanabe, C. Minami, H. Koike, S. Itoh, Y. Kashino, K. Satoh, I. Photosystem, complexes associated with fucoxanthin-chlorophyll-binding proteins from a marine centric diatom, *Chaetoceros gracilis*, Biochim. Biophys. Acta 1777 (2008) 351–361.
[53] T.A. Roelofs, C.H. Lee, A. Holzwarth, Global target analysis of picosecond chlorophyll fluorescence kinetics from pea chloroplasts, a new approach to the characterization of the primary processes in photosystem II alpha- and beta-units, Biophys. J. 61 (1992) 1147–1163.
[54] Y. Miloslavina, M. Szczepaniak, J. M G Müller, M. Sander, M. Nowaczyk, A.R. Rögner, Holzwarth, Charge separation kinetics in intact photosystem II core particles is trap-limited. A picosecond fluorescence study, Biochem. 45 (2006) 2436–2442.
[55] K. Broess, G. Trinkunas, C.D. van der Weij-de Wit, J.P. Dekker, A. van Hoek, H. van Amerongen, Excitation energy transfer and charge separation in photosystem II membrane revisited, Biophys. J. 91 (2006) 3776–3786.
[56] S. Vassiliev, C.I. Lee, G.W. Brudvig, D. Bruce, Structure-based kinetic modeling of excited-state transfer and trapping in histidine-tagged PS II core complexes from *Synechocystis*, Biochem. 41 (2002) 12236–12243.
[57] G. Raszewski, T. Renger, Light harvesting in photosystem II core complexes is limited by the transfer to the trap: can the core complex turn into a photoprotective mode? J. Am. Chem. Soc. 130 (2008) 4431–4446.